Molecular Vision 2016; 22:953-958 <http://www.molvis.org/molvis/v22/953>
Received 16 August 2015 | Accepted 3 August 2016 | Published 5 August 2016

Technical brief: Pump-probe paradigm in an integrating cavity to study photodecomposition processes

Federico Gonzalez-Fernandez,[1,2] Brandi Betts-Obregon,[3] Andrew T. Tsin,[3] Richard J. DeSa[4]

[1]Departments of Ophthalmology and Pathology, University of Mississippi Medical Center, Jackson, MS; [2]Research & Development Service, G.V. (Sonny) Montgomery Veterans Affair Medical Center, Jackson, MS; [3]Department of Biology, The University of Texas at San Antonio, San Antonio, TX; [4]OLIS, Inc. Bogart, GA

Purpose: Assaying photodecomposition is challenging because light must be used to initiate the photodamage and light must be used to monitor the photodecomposition. The experimental requirements are as follows: 1) During exposure of the actinic beam, continuously monitor the spectral characteristics of the sample, 2) uniformly expose the reactants to the actinic source, 3) obtain informative spectra in the presence of light scatter, and 4) achieve sufficient sensitivity for dilute reactants. Traditional spectrophotometers cannot address these issues due to sample turbidity, the inability to uniformly expose the cuvette contents to the incident beam, the inability to simultaneously perform spectral scans, and inherent low sensitivity. Here, we describe a system that meets these challenges in a practical way.

Methods: Light access to a 8.6 ml quartz integrating sphere containing 10 µM all-*trans* retinol in PBS was provided by three ports at right angles allowing for the following: 1) actinic light delivery from light-emitting diodes (LEDs) firing at 100 pulses/sec, 2) entry of a separate scanning beam at 100 scans/sec (10,000 µsec scan time) via an OLIS RSM 1000 ultraviolet/visual (UV/Vis) rapid-scanning spectrophotometer (RSM), and 3) light exit to the detector photomultiplier. The RSM spectral intermediate slit was partially covered to allow for a "dark" period of 2,000 µsec when no scanning light was admitted to the cuvette. During that interval, the LED was flashed, and the photomultiplier was temporarily blocked by a perforated spinning shutter disk. The absorbance per centimeter, which is increased due to the internal reflectance of the integrating sphere compared to a standard 1 cm rectangular cuvette, was calculated according to Fry *et al*. (2010) *Applied Optics* 49:575. Retinoid photodecomposition was confirmed with high-performance liquid chromatography (HPLC).

Results: Using the RSM to trigger the LED flash and photomultiplier shutter closure during the "dark" period allowed actinic flashes to be placed between scans. Exposure of the all-*trans* retinol to 366 nm flashes resulted in marked reduction in absorbance and a blue shift of the λ_{max}. A white LED, despite its higher photon output, did not support all-*trans* retinol photolysis. Singular value decomposition (SVD) analysis revealed three spectral intermediates with mechanism, I -> II -> III. HPLC analysis of the reactants at the beginning and the conclusion of the light exposure confirmed the retinol photodecomposition.

Conclusions: The highly reflecting cavity acts as a multipass cuvette that markedly increased the light path length and, thus, sensitivity. Triggering the LED during a dark period within the scan time allowed the actinic flashes to be interleafed between scans in a pump-probe paradigm. Furthermore, the entire sample was exposed to scan beam and actinic flashes, which is not possible in traditional spectrophotometers. Finally, the integrating cavity cuvette allowed use of turbid samples. SVD was useful for resolving spectral intermediates. Although the identity of the intermediates was not determined here, the ability to define molecular intermediates during photodecomposition reactions will allow future studies to isolate and identify the degradation products and determine the mechanism of light-induced retinoid degradation and that of retinoid-binding protein-mediated photoprotection.

We have been intrigued by the ability of interphotoreceptor retinoid-binding protein (IRBP) to protect visual cycle retinoids from photodegradation [1] and IRBP's free radical scavenging activity [2]. Therefore, we sought a platform to study the mechanism(s) of these important biochemical activities. Furthermore, as ongoing X-ray crystallographic studies are providing valuable information regarding the retinoid and fatty-acid binding sites of the protein, biochemical studies are needed to evaluate functional mechanisms suggested from new structural information [3-6].

Designing biochemical assays of retinoid photodecomposition is challenging because light must be used to initiate the photodamage, and light is also needed to monitor the photodecomposition. There are four experimental challenges to address. First, such assays require exposure of the sample to the actinic light while simultaneously monitoring its

Correspondence to: Federico Gonzalez-Fernandez, Associate Chief of Staff for Research & Development, G.V. (Sonny) Montgomery Veterans Affairs Medical Center, Research & Education Building, Room 312, 1500 East Woodrow Wilson Drive, Jackson, Mississippi 39216; Phone: (716) 863-2291; FAX: (601) 364-1390; email: FGonzalezfernandez@umc.edu

changing spectral characteristics. Second, a cuvette system is required where uniform exposure of reactants to the actinic source can be achieved. Third, the interference of light scatter common in biologic materials must be mitigated especially when dealing with cloudy specimens such as cellular suspensions. Finally, high sensitivity is required particularly with limited specialized reagents and the production of transient intermediates. Traditional spectrophotometers using single-pass rectangular cuvettes cannot address these issues due to light scattering, the inability to uniformly expose the cuvette contents to the incident light beam, and low sensitivity. Here, we describe the application of rapid scanning spectroscopy with an integrating cavity to meet these challenges in the context of retinoid photodecomposition.

METHODS

Chemicals: All reagents were of the highest purity and obtained from Sigma-Aldrich (St. Louis, MO), unless otherwise specified. The purity of all-*trans* retinol was >99.0% according to high-performance liquid chromatography (HPLC). Stock solutions were prepared fresh in 100% ethanol in a 30 ml amber glass vial with Teflon-lined lids. The all-*trans* retinol concentration was determined with absorbance spectroscopy using an extinction coefficient of 38,300 M/cm (in ethanol) [7]. HPLC-grade solvents were purchased from Fisher Scientific Co. (Springfield, NJ). For photodecomposition assays, the retinol was dispersed in PBS (137 mM NaCl, 2.7 mM KCl, 10 mM PO_4^{-3}, pH 7.4)

Rapid scanning spectrophotometer with integrating cavity: The photodecomposition study used a rapid scanning spectrophotometer (RSM 1000) fitted with a quartz-integrating cavity as the sample cuvette (CLARiTY 1000, Online Instrument Systems, Inc., Bogart, GA). The cavity, which holds a sample volume of 8.6 ml, was encased in a highly reflective chamber, so that the light entering remains within to maximize diffuse reflectance of light off the exterior walls of the flask. This chamber, the DeSa Suspension Presentation Cavity (DSPC), is equipped with four lateral light ports (Figure 1). A central superior port allows introduction of the sample into the DSPC, which is continuously stirred with a magnetic stir bar at ambient temperature. Scanning light (300 to 510 nm) is delivered using the double monochromator, capable of rapid-scanning at 100 spectra scans/second. The apertures to the reflecting sphere through which the measuring light entered and the transmitted and scattered light exited to the photomultiplier tube were at 90° angles to each other. The contents of the DSPC were exposed to the actinic light using light-emitting diodes (LEDs) inserted into the third port. The LEDs used had peak outputs shown in Figure 2.

The system is designed to expose all-*trans* retinol to an actinic light while simultaneously monitoring its photodecomposition spectroscopically in real time. This is accomplished by interleafing the spectral scans with the actinic flashes as illustrated in Figure 1. The moving slit from the RSM spinning disk generates 100 spectral scans per second (Figure 1A). A fixed light-block creates a dark period within each scan (Figure 1B). During this period, the LED is triggered to flash, and the photomultiplier shutter is temporarily closed. Alternating LED flashes with spectral scans allows a pump-probe paradigm. The three-dimensional data were subjected to singular value decomposition (SVD) [8]. Raw apparent absorbance values were converted to absorbance values per centimeter as previously described [9,10].

HPLC analysis: Retinols were transferred and processed for HPLC analyses under dim red light. Following light exposure, the aqueous sample was removed from the DSPC and extracted three times with an equal volume of cold ethanol and two volumes of hexane followed by centrifugation at 1500 ×*g* at 5 °C for 3 min. Samples were then dried under nitrogen and immediately analyzed using an HPLC system equipped with a ZORBAX normal-phase Rx-SIL 5 µm, 4.6 mm × 250 mm column (Agilent Technologies, Santa Clara, CA) and an online 2996 photodiode array detector run by Empower software (Waters Technologies, Milford, MA). The HPLC column was subjected to 10% dioxane in hexane at a flow rate of 1.0 ml/min, and the eluent monitored at 318 nm. Retinols were identified by comparison with the retention times of authentic standards and their online ultraviolet (UV) spectra with absorbance maxima at 318 and 325 nm for 11-*cis* and all-*trans* retinols, respectively.

RESULTS

To allow for a "pump-probe" paradigm, where the effects of photolysing actinic light on the sample can be followed in real time, trigger signal from the RSM was used to synchronize the actinic LED flashes and the photomultiplier shutter. The RSM provided 100 spectral scans/sec, or 10,000 µsec/scan. For 2,000 µsec, the scanning light was blocked creating a "dark" interval where the LED was flashed and the photomultiplier was temporarily protected by the shutter.

The incoming scan beam from the rapid scanning UV/visible spectrophotometry (Vis) monochromator is split between reference and sample DSPCs providing a dual-beam configuration, allowing compensation for light fluctuations. Within each compartment, traditional single-pass rectangular cuvettes are replaced with spherical quartz DSPC cuvettes. In the configuration shown in Figure 1, the incoming spectral scans enter the integrating cavity through a port opposite the

LED that provides the actinic light. The spectral output of the LEDs is shown in Figure 2. The 366 nm LED was used for photodecomposition studies due to its good output in the UVA region. The cuvettes were surrounded by a reflective material that fully scattered the measurement beam and monochromatic LED flashes. The highly reflecting cavity therefore acts as a multipass cuvette. The effective path length is markedly increased (tens of centimeters) compared to rectangular single-pass cuvettes. Because of this property, the entire sample within the integrating cavity is exposed to the actinic light unlike the situation in traditional cuvettes. Finally, although not relevant to the measurement made in this report, light scatter by the specimen is completely mitigated [9,11-13].

The system allows retinol photodecomposition to be followed through rapid spectral scans interleafed between the LED flashes (Figure 3). One hundred scans were taken per second for 5,000 s. The actinic LED peak output was 366 nm driven at 100 flashes/sec. Note the marked reduction in absorbance with blue shift of the λ_{max}. The white LED, despite its higher output (Figure 2), did not support all-*trans* retinol photolysis. The absorbance data were corrected to take into account the increased light path length due to the multiple internal reflections (R = 0.92 [10]; note the change in the absorbance scales between Figure 3 and Figure 4A,B). The three-dimensional data were subjected to SVD [8] (Figure 4). Three spectral intermediates were resolved indicated by the purple, blue, and green tracings representing species I, II, and III, respectively. SVD analysis favored a reaction mechanism: I -> II -> III. Note the excellent fit of the decay plot to the data (black tracing in Figure 4B), and the residuals plot further confirming the fit accuracy (Figure 4D). HPLC analysis of the reactants at the beginning (blue) and the conclusion of

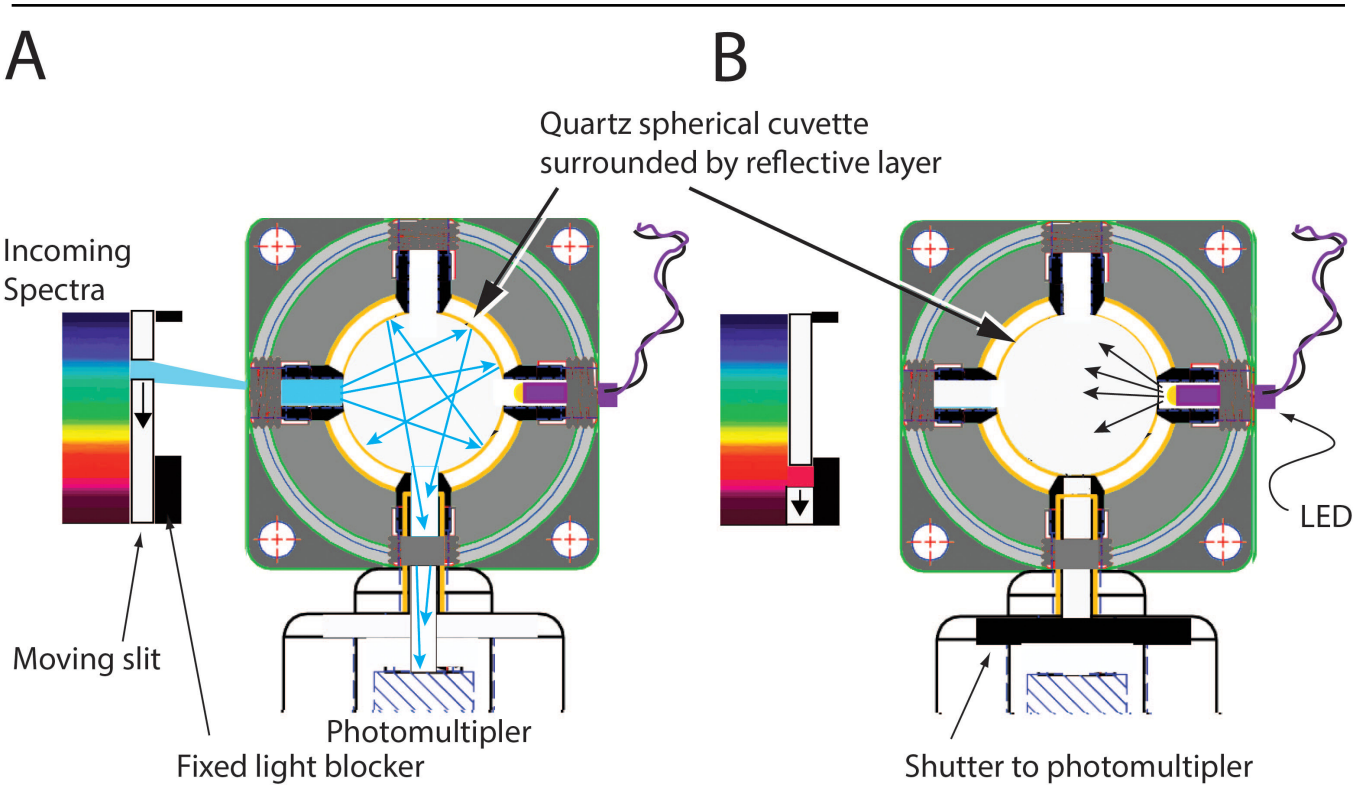

Figure 1. RSM with integrating cavity absorption meter and actinic LED source. **A**: Scan phase: The moving slit from the rapid-scanning spectrophotometer (RSM) creates spectral scans at a rate of 100 scans per second. Light from the RSM is split to each of the cuvette compartments (not illustrated). There, conventional single-pass rectangular cuvettes are replaced with spherical quartz cuvettes (DeSa Spherical Presentation Chambers, DSPCs). Each DSPC is surrounded by four light ports. In the present configuration, the incoming light enters through the port opposite the light-emitting diode (LED). The photomultiplier port is positioned at right angles to both. The spherical cuvette is surrounded by a reflective material fully scattering the measurement beam as well as the monochromatic light from the LED. The highly reflecting cavity acts as a multipass cuvette. The effective path length is markedly increased (tens of centimeters) compared to traditional single-pass cuvettes, and effects of light scatter are eliminated. **B**: Actinic exposure pulse: A fixed light block creates a dark period within each scan. During this period, the LED is triggered to flash, and the photomultiplier shutter is temporarily closed. By interleafing scans with LED flashes, light-induced chemical changes can be followed spectroscopically in real time.

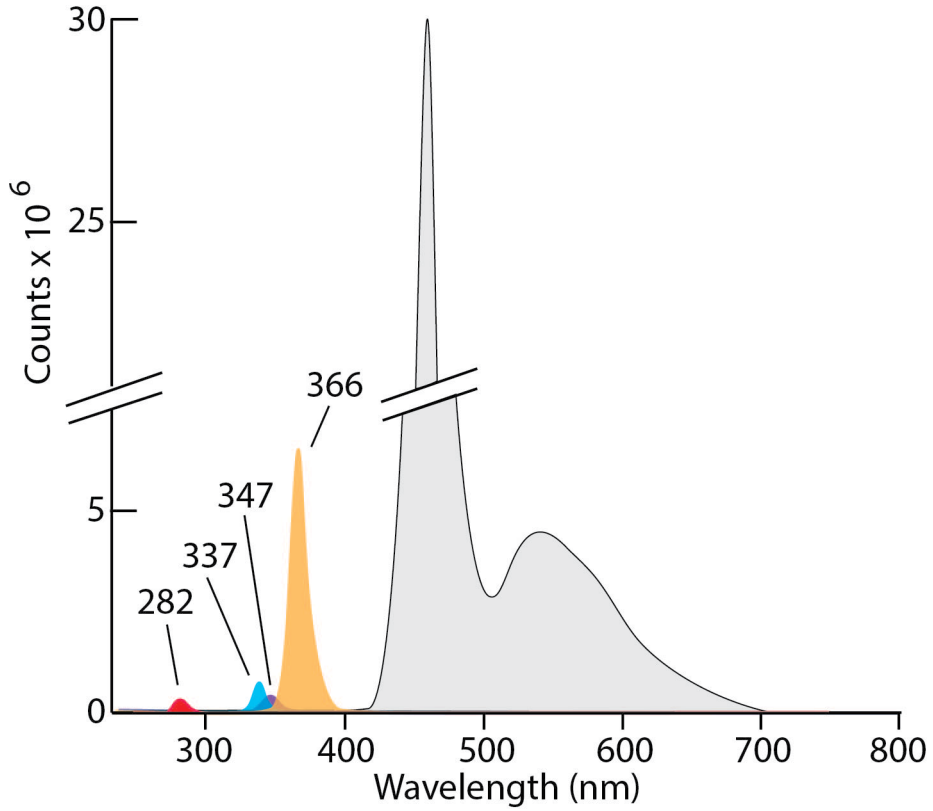

Figure 2. Spectral output of the actinic light-emitting diodes (LEDs). LEDs can be placed individually within the DeSa Suspension Presentation Cavity (DSPC) port as shown in Figure 1.

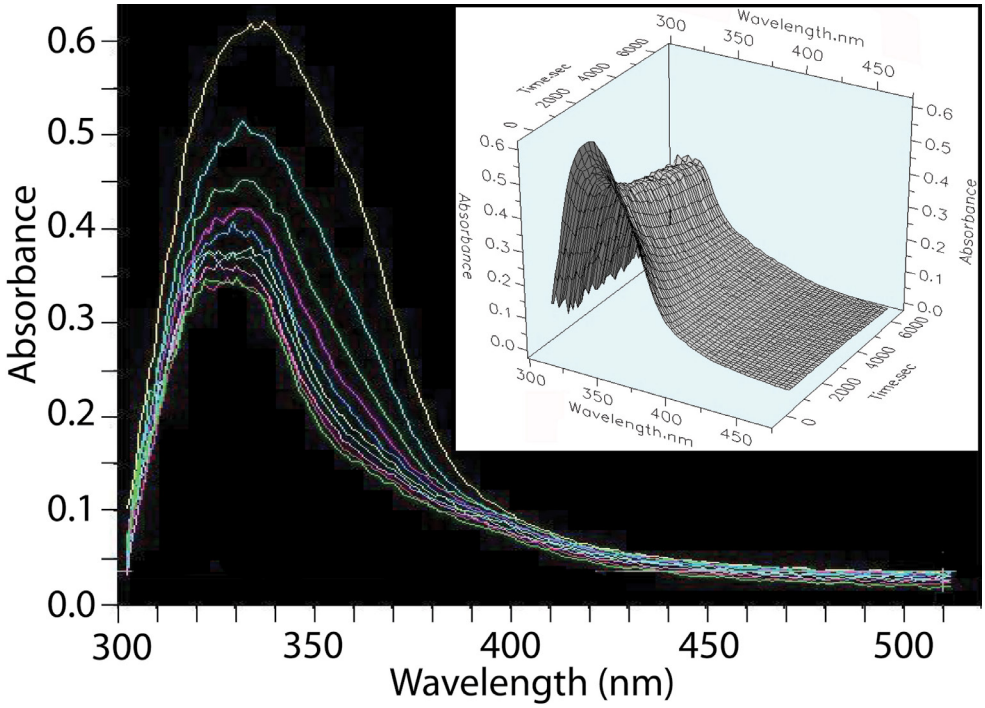

Figure 3. Photodecomposition of all-*trans* retinol followed through rapid spectral scans interleafed between the actinic LED flashes. The all-*trans* retinol concentration was 10 µM in 8.6 ml of PBS, pH 7.4. Retinol likely existed as a combination of monomers, multimers, and micelles. Nevertheless, each form would be exposed to the actinic light. One hundred scans are taken per second for 5,000 s. Scans were averaged to two scans per second. Ten such averaged scans are shown (one scan per minute). The actinic light-emitting diode (LED) peak output was 366 nm driven at 100 flashes/sec. The insert shows the data in three-dimensional representation.

the light exposure (red) confirmed the photodecomposition of all-*trans* retinol.

DISCUSSION

We sought a platform to study visual cycle retinoid photodecomposition and the mechanism of its photoprotection by retinoid-binding proteins [1]. However, studying such photodecomposition reactions presents several experimental challenges that require the following: 1) simultaneous exposure to the actinic light while simultaneously monitoring spectral characteristics, 2) ensuring uniform exposure of reactants to the actinic source, 3) mitigation of light scatter common in turbid biologic materials, and 4) adequate sensitivity. Here, we found that rapid scanning spectroscopy using an integrating quartz cavity in coordination with an LED flash source can meet these experimental challenges.

We described a pump-probe paradigm, where photodecomposition can be followed in real time. This was accomplished using a trigger from the RSM to synchronize the LED flashes and the photomultiplier's shutter. The Olis RSM delivered 100 scans/sec with a 2,000 µsec "dark" interval. During this interval, the LED was flashed while the photomultiplier was simultaneously blocked with a synchronized spinning disk shutter. A key innovation was replacing the traditional single-pass rectangular cuvette with a spherical quartz-integrating cavity. The cuvette was surrounded by a reflective material that fully scattered the measurement beam and monochromatic LED flashes. Therefore, the highly reflecting cavity acted as a multipass cuvette. The effective path length was markedly increased (tens of centimeters) compared to rectangular single-pass cuvettes. Because of this property, the entire sample within the integrating cavity was exposed to the actinic light unlike the situation in traditional cuvettes.

Finally, although not relevant to the measurements made in this report, specimen light scatter can be effectively eliminated [9,11-13]. The integrating cavity described here allows informative spectra to be obtained in cloudy suspensions not suitable for single-pass rectangular cuvettes. We

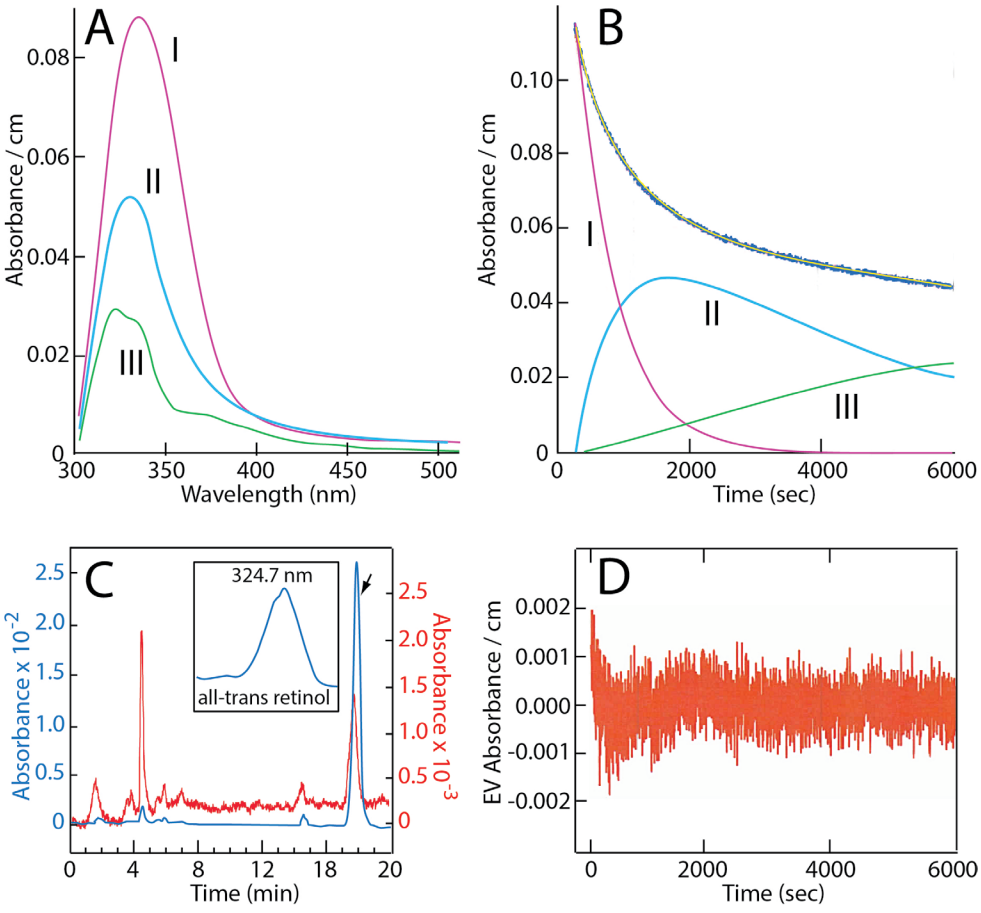

Figure 4. Kinetic analysis and HPLC confirmation of retinol photodecomposition. **A**: The three-dimensional data from the previous figure were corrected for the increased path length and subjected to singular value decomposition (SVD). Three spectral intermediates are resolved indicated by the purple, blue, and green intermediates representing species I, II, and III, respectively. **B**: The analysis favors a reaction mechanism: I -> II -> III. **C**: High-performance liquid chromatography (HPLC) analysis of the reactants at the beginning (blue) and the conclusion of the light exposure (red; note that red chromatogram is displayed at tenfold higher gain compared to the blue profile). The mobile phase consisted of 10% dioxane in hexane (1.0 ml/min) monitored at 318 nm. In line spectral analysis of the peak, with λ_{max} = 324.7 nm (arrow, prelight exposure) is consistent with all-*trans* retinol. The 16 min peak = 13-*cis* retinol. **D**: Residual plot confirms the fit accuracy.

have reported that the use of this technology allows obtaining rhodopsin spectra in crude outer segment preparations and dispersed retina and whole retina preparations [14,15]. SVD was useful for resolving the kinetics of spectral intermediates [6]. The identity of the spectral intermediate(s) cannot be determined from the present data but may include a combination of photodegradation and photoisomerization products. The system described here could be extended to photodecomposition of retinoids [16] and A2E [17]. Finally, the instrumentation described here will allow future studies to determine the mechanism of IRBP-mediated photoprotection [1].

ACKNOWLEDGMENTS

The authors thank Julie Ann DeSa Lorenz and Dr. Paul Boxrud (Olis, Inc.) for helpful discussions. This work was funded in part by NIH RO1EY09412 (F.G.-F.), a Merit Review Award I01BX007080 from the Biomedical Laboratory Research & Development Service of the Veterans Affairs Office of Research and Development (F.G.-F.), Start-up Award from Research Mississippi, Inc (F.G.-F.), and a grant from the National Institute on Minority Health and Health Disparities (G12MD007591) (A.T.T.).

REFERENCES

1. Gonzalez-Fernandez F, Betts-Obregon B, Yust B, Mimun J, Sung D, Sardar D, Tsin AT. Interphotoreceptor retinoid-binding protein protects retinoids from photodegradation. Photochem Photobiol 2015; 91:371-8. [PMID: 25565073].
2. Gonzalez-Fernandez F, Sung D, Haswell KM, Tsin A, Ghosh D. Thiol-dependent antioxidant activity of interphotoreceptor retinoid-binding protein. Exp Eye Res 2014; 120:167-74. [PMID: 24424263].
3. Gonzalez-Fernandez F, Bevilacqua T, Lee KI, Chandrashekar R, Hsu L, Garlipp MA, Griswold JB, Crouch RK, Ghosh D. Retinol-binding site in interphotoreceptor retinoid-binding protein (IRBP): a novel hydrophobic cavity. Invest Ophthalmol Vis Sci 2009; 50:5577-86. [PMID: 19608538].
4. Loew A, Gonzalez-Fernandez F. Crystal structure of the functional unit of interphotoreceptor retinoid binding protein. Structure 2002; 10:43-9. [PMID: 11796109].
5. Ghosh D, Haswell K, Sprada M, Gonzaez-Fernandez F. Structure of zebrafish IRBP reveals its fatty acid-binding. Exp Eye Res 2015; 140:149-58. [PMID: 26344741].
6. Ghosh D, Haswell K, Sprada M, Gonzaez-Fernandez F. Fold Conservation and Proteolysis in Zebrafish IRBP Structure: Clues to Possible Enzymatic Function? Exp Eye Res 2016; 147:78-84. [PMID: 27155144].
7. Szuts EZ, Harosi FI. Solubility of retinoids in water. Arch Biochem Biophys 1991; 287:297-304. [PMID: 1898007].
8. DeSa RJ, Matheson IB. A practical approach to interpretation of singular value decomposition results. Methods Enzymol 2004; 384:1-8. [PMID: 15081677].
9. Javorfi T, Erostyak J, Gal J, Buzady A, Menczel L, Garab G, Razi Naqvi K. Quantitative spectrophotometry using integrating cavities. J Photochem Photobiol B 2006; 82:127-31. [PMID: 16307890].
10. Fry ES, Kattawar GW, Strycker BD, Zhai PW. Equivalent path lengths in an integrating cavity Appl Opt 2010; 49:575-7. comment[PMID: 20119003].
11. Erostyak J, Javorfi T, Buzady A, Naqvi KR, Garab G. Comparative study of integrating cavity absorption meters. J Biochem Biophys Methods 2006; 69:189-96. [PMID: 16644020].
12. Fry ES, Kattawar GW, Pope RM. Integrating cavity absorption meter. Appl Opt 1992; 31:2055-65. [PMID: 20720859].
13. Elterman P. Integrating cavity spectroscopy. Appl Opt 1970; 9:2140-2. [PMID: 20094211].
14. Gonzalez-Fernandez FD. R. A novel approach to demonstrating rhodopsin regeneration in living cellular suspensions and detached intact retina by mitigating light scatter. ARVO Annual Meeting; 2015 May 3-7; Denver, CO.
15. Gonzalez-Fernandez FDR. How to obtain a rhodopsin spectrum of a cellular suspension - beating the light scatter problem. ARVO Annual Meeting; 2014 May 4-8; Orlando, FL.
16. Tolleson WH, Cherng SH, Xia Q, Boudreau M, Yin JJ, Wamer WG, Howard PC, Yu H, Fu PP. Photodecomposition and phototoxicity of natural retinoids. Int J Environ Res Public Health 2005; 2:147-55. [PMID: 16705812].
17. Wu Y, Yanase E, Feng X, Siegel MM, Sparrow JR. Structural characterization of bisretinoid A2E photocleavage products and implications for age-related macular degeneration. Proc Natl Acad Sci USA 2010; 107:7275-80. Epub 2010 Apr 5[PMID: 20368460].

Articles are provided courtesy of Emory University and the Zhongshan Ophthalmic Center, Sun Yat-sen University, P.R. China. The print version of this article was created on 5 August 2016. This reflects all typographical corrections and errata to the article through that date. Details of any changes may be found in the online version of the article.